

# Ultra-fine Particulate Detection using Mode-localized MEMS Resonators

Malar Chellasivalingam<sup>1</sup>, Milind Pandit<sup>1</sup>, Markus Kalberer<sup>2</sup>, Ashwin A. Seshia<sup>1</sup>

<sup>1</sup>The Nanoscience Centre, Department of Engineering, University of Cambridge, UK

<sup>2</sup>Centre for Atmospheric Science, Department of Chemistry, University of Cambridge, UK  
mc2076@eng.cam.ac.uk

**Abstract** — This paper demonstrates the feasibility of employing mode localized mass sensing in coupled MEMS resonators for ultra-fine particulate detection applications. The potential benefits of this approach include higher parametric sensitivity compared to the resonant frequency shift-based detection approach. Weakly coupled MEMS resonators demonstrated in this paper demonstrate sensitivity to fine particulates and a significant improvement in mass sensitivity for particulate quantification by employing an amplitude ratio shift output metric.

**Keywords**—ultra-fine particulate matter; mode localization; amplitude ratio; coupled MEMS resonators; mass sensor; Lamé mode; piezoelectric bulk acoustic resonators

## I. INTRODUCTION

Airborne Particulate Matter (PM) that often arise from dust, smoke, carbon emissions in diesel engines etc. are termed as one of the harmful pollutants causing respiratory and cardiovascular diseases. A large number of studies have demonstrated the significant relative health impact mainly due to ultra-fine PM, corresponding to particles less than 100nm in diameter. In order to detect these ultra-fine particles and thereby to monitor their emission sources, optical methods are often employed due to their high temporal resolution and their ability to count individual particles. At the length scale below 100nm, however, optical methods are limited for PM detection and can only be employed indirectly as a measure of PM concentration due to the diffraction limit [1].

Hence, MEMS resonators have been researched as a means of detecting ultra-fine PM based on the frequency shift sensing approach considering the high mass sensitivity, small size and low cost. In addition, the miniaturization and large-scale volume manufacturing offered by the MEMS resonators makes them suitable for developing portable sensors that can be deployed as population-based exposure assessment tools. Researchers so far have employed different topologies of MEMS resonators with different particulate matter collection approaches to develop portable sensors. Black et al. [2] used thin-film bulk acoustic resonators with thermophoresis to detect particles while Mehdizadeh et al. [3] used thermally actuated micro resonators combined with inertial impaction. Wasisto et al. [4,5] used flexural mode silicon cantilevers employing electrostatic

collection of particles. On the other hand, Zeilinski et al. [1] used piezoelectric bulk acoustic resonators combined with inertial impaction technique. In all these approaches, resonant frequency shift was used as the output metric for the particulate matter deposited on the resonators. However, MEMS resonators can potentially exhibit significant drift in resonant frequency due to temperature fluctuations and other environmental effects, limiting long term measurements required for PM detection [1].

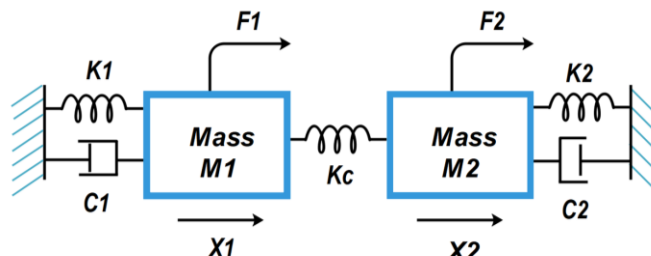


Fig. 1. Mass spring damper representation of two degrees of freedom resonator system

In this research paper, we have employed weakly-coupled piezoelectric square plate bulk acoustic MEMS resonators due to their innate ability for common mode rejection [6-9]. Such systems can then exploit vibration mode localization as a measure of structural asymmetry induced by mass loading which in turn makes them highly sensitive to ultra-fine PM. Since impactors are known to minimally influence the physical properties (temperature and charge) of the particles [1], we have chosen inertial impaction as the particle collection approach. In addition, the square plate bulk acoustic resonator topology employed in this work offers large surface area for particulate deposition with demonstrated high Quality factors in air when operated in higher order in-plane bulk modes [10].

By establishing ultra-fine particulate matter sensing using this weakly-coupled resonator topology, an approximately three orders of magnitude improvement in sensitivity compared to frequency shift sensing using the same configuration is shown. The amplitude ratio shift in the coupled resonators is used as the output metric for demonstrating this sensitivity improvement.

## II. MODE LOCALISATION: THEORY

The mode localization phenomenon can be modeled using a simple discrete model of a two degrees of freedom resonator system. The two masses (mass M1 and mass M2) as shown in

Fig. 1. represent the intrinsic masses of the two resonators and the two springs (K1 and K2) represent their corresponding stiffnesses. The coupling spring stiffness is represented by Kc and it is assumed to be far weaker than the springs of the resonators themselves. The damping associated with the two masses is represented by C1 and C2. Similarly, X1 and X2 denote the displacement of the resonators whereas F1 and F2 denote the force applied on the individual resonators.

The equations of motion are for this 2DoF system are:

$$m_1\ddot{x}_1 + c_1\dot{x}_1 + k_1x_1 + k_c(x_1 - x_2) = F_1 \quad (1)$$

$$m_2\ddot{x}_2 + c_2\dot{x}_2 + k_2x_2 + k_c(x_2 - x_1) = F_2 \quad (2)$$

By applying Laplace Transform to the equations of motion, we obtain

$$X_1(s)[M_1s^2 + C_1s + K_1 + K_c] = F_1(s) + K_c X_2(s) \quad (3)$$

$$X_2(s)[M_2s^2 + C_2s + K_2 + K_c] = F_2(s) + K_c X_1(s) \quad (4)$$

$$\text{where, } H_1(s) = M_1s^2 + C_1s + K_1 + K_c \quad (5)$$

$$H_2(s) = M_2s^2 + C_2s + K_2 + K_c \quad (6)$$

Rearranging the above equations, we get

$$X_1(s)H_1(s) - K_cX_2(s) = F_1(s) \quad (7)$$

$$X_2(s)H_2(s) - K_cX_1(s) = F_2(s) \quad (8)$$

Using Cramer's rule, the displacement of individual resonators with respect to the individual forces applied can be derived as follows [11].

$$X_1(s) = \frac{H_2(s)F_1(s) + K_cF_2(s)}{H_1(s)H_2(s) - K_c^2} \quad (9)$$

$$X_2(s) = \frac{H_1(s)F_2(s) + K_cF_1(s)}{H_1(s)H_2(s) - K_c^2} \quad (10)$$

In general, the transfer function of the displacement of resonator  $i$  due to the force on resonator  $j$  can be expressed as given in [11].

$$X_i = \sum_{j=1}^2 H_{ij}F_j \quad (11)$$

In the 2 DoF coupled resonator system shown in Fig.1., if we assume the following conditions

- (i)  $M_1 = M, M_2 = M + \Delta M, K_1 = K_2 = K, C_1 = C_2 = C,$
- (ii) resonators are weakly coupled by satisfying  $K_c \ll K,$
- (iii) the force is applied only from one side such that  $F_1 = F,$  and  $F_2 = 0,$

then the transfer function of the 2DoF coupled resonator system can be rewritten from (9) and (10) as,

$$X_1(s) = \frac{H_2(s)}{H_1(s)H_2(s) - K_c^2} F(s) \quad (12)$$

$$X_2(s) = \frac{K_c}{H_1(s)H_2(s) - K_c^2} F(s) \quad (13)$$

Equations (12) and (13) provide the amplitude of displacement of the resonators 1 and 2 respectively, for the applied force F.

This simply means that at the initial state, the system was symmetric, and the two masses were assumed to be identical. When asymmetry is created in the system by introducing a slight perturbation in mass ( $\Delta M$ ) in one of the resonators (in this case, mass M2), the modes localize. Therefore, the vibration energy will be confined to one of the resonators instead of being equally divided between the two resonators when at their initial state. This phenomenon is called mode localization. The advantage of mode localisation will be evident if we consider the amplitude ratio shift between the two coupled resonators instead of frequency shift.

The modal frequencies and amplitude ratio at each mode for the coupled resonators can then be expressed as,

$$\omega_1^2 = \frac{(K + K_c)(\Delta M + 2M) - \sqrt{\Delta M^2(K + K_c)^2 + 4MK_c^2(\Delta M + M)}}{2M(\Delta M + M)} \quad (14)$$

$$\left| \frac{X_1}{X_2} \right|_{\omega_1} = -\frac{1}{2} \left[ \frac{\Delta M(K + K_c) - \sqrt{\Delta M^2(K + K_c)^2 + 4MK_c^2(\Delta M + M)}}{K_c(\Delta M + M)} \right] \quad (15)$$

$$\omega_2^2 = \frac{(K + K_c)(\Delta M + 2M) + \sqrt{\Delta M^2(K + K_c)^2 + 4MK_c^2(\Delta M + M)}}{2M(\Delta M + M)} \quad (16)$$

$$\left| \frac{X_1}{X_2} \right|_{\omega_2} = -\frac{1}{2} \left[ \frac{\Delta M(K + K_c) + \sqrt{\Delta M^2(K + K_c)^2 + 4MK_c^2(\Delta M + M)}}{K_c(\Delta M + M)} \right] \quad (17)$$

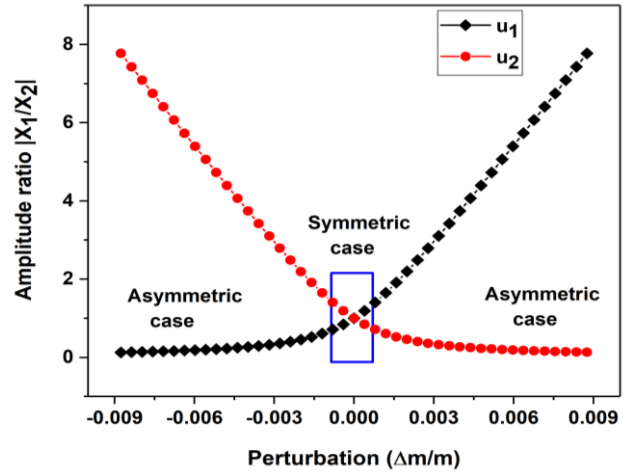


Fig. 2. Theoretical simulation of amplitude ratio in the coupled system by introducing a slight mass perturbation in one of the resonators

From Fig. 2. it is evident that under asymmetric condition created by a slight mass perturbation in one of the resonators, the vibration energy is confined to one of the modes in the

resonators and the amplitude ratio between the resonators is a good representation of such vibration energy confinement.

### III. WEAKLY COUPLED MEMS RESONATORS : DESIGN

Two square plate piezoelectric bulk acoustic resonators operating at their in-plane Lamé mode were designed to exhibit mode localization. The square plate resonators were fixed at their four corners by T-shaped anchors. A short mechanical beam was used as a coupler connecting the two resonators at their nodal points to maximize the effects of mode localization by providing weak-coupling. Fig. 3. and Fig. 4. shows the COMSOL simulation of the symmetrical (unperturbed) and asymmetrical (perturbed) anti-phase Lamé modes that were measured in the square plate resonator respectively. In simulation, by adding a fixed mass on the resonator 1, the phenomenon of mode localization was observed in resonator 1 with respect to resonator 2 as shown in Fig 4.

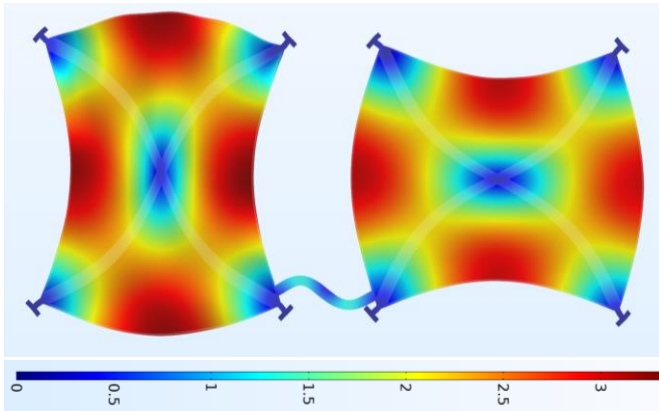


Fig. 3. Symmetrical (unperturbed) weakly coupled resonators exhibiting out-of-phase Lamé mode (~2.5 MHz)

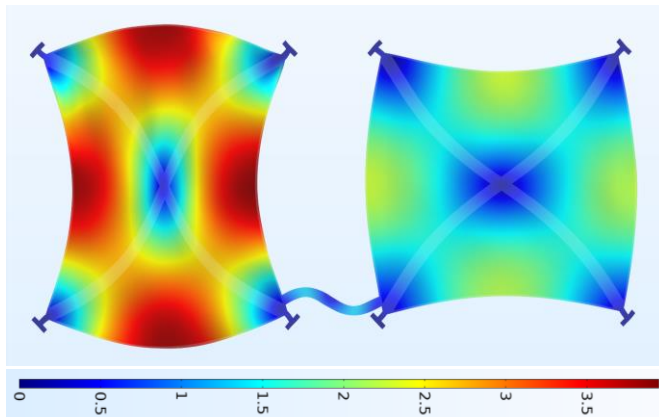


Fig. 4. Asymmetrical (perturbed) weakly coupled resonators exhibiting out-of-phase Lamé mode (~2.5 MHz)

The coupled resonators were then fabricated using silicon-on-insulator (SOI) wafers via a five-mask modified industrial Multi-user MEMS process (MUMPs) by MEMSCAP Inc. The process involved reactive sputtering of  $0.5\mu\text{m}$  thin AlN layer, deposition of  $1\mu\text{m}$  Cr/Al metal electrodes and subsequent

release of the structure using deep-reactive ion etching process as explained in [12]. The fabricated weakly-coupled resonators were characterized by driving the resonator 1 using differential actuation at its in-plane Lamé mode (~2.5 MHz) and the frequency response was observed from both the resonators (1&2) individually.

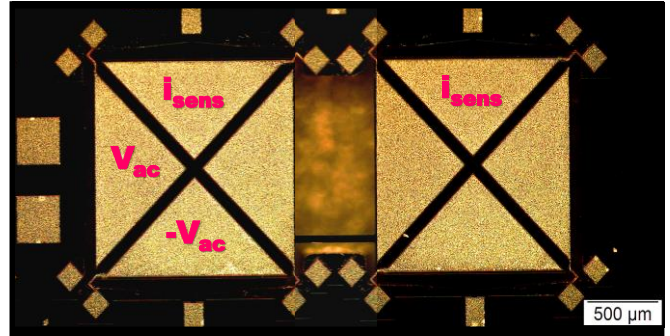


Fig. 5. Dark-field microscopic image of the fabricated weakly coupled piezoelectric bulk acoustic MEMS resonators

### IV. EXPERIMENTAL SET-UP

To verify vibration mode localization in the weakly coupled piezoelectric bulk acoustic resonators, and to demonstrate their ultra-fine particulate sensitivity, a simple experimental set-up was designed.

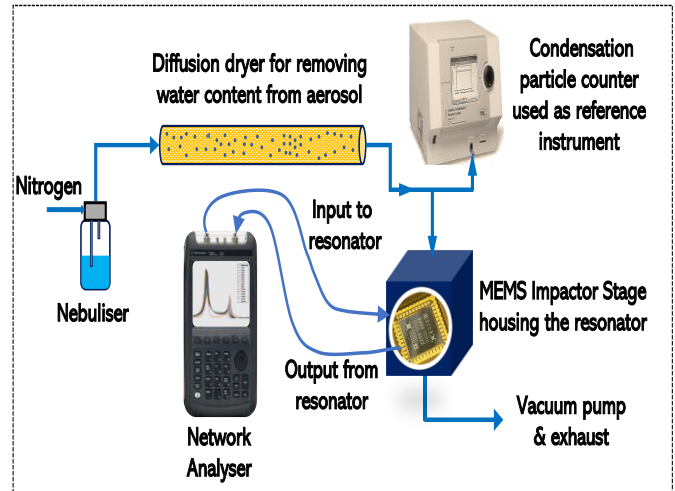


Fig. 6. Experimental set-up for depositing ultra-fine PSL particles on weakly coupled MEMS resonators

The experimental setup consists of a MEMS Impactor Stage (MIS) connected to a particle generation arrangement as shown in Fig. 6. The Polystyrene Latex (PSL) particles of around  $296 \pm 6\text{nm}$  in diameter were treated as model ultra-fine PM. By passing nitrogen gas over a suspension containing the mixture of ultra-fine PSL particles in a High-Performance Liquid Chromatography (HPLC)-grade water, the ultra-fine particles were nebulized. These particles were then fed through a diffusion dryer filled with silica gel to remove their water

content and were deposited on the weakly-coupled MEMS resonators by means of inertial impaction. The flow rate for the generated PSL particles was fixed at 2.17 L/min such that the particle concentration was maintained at approximately  $7.96 \times 10^2$  particles/cm<sup>3</sup> throughout the time period of deposition. The particle loss during deposition was assumed to be negligible. A condensation particle counter (CPC) was used as a reference instrument for recording the particle concentration during deposition. The frequency response of the coupled resonators was measured using a Network Analyser (N9915A, Agilent) in an open-loop configuration.

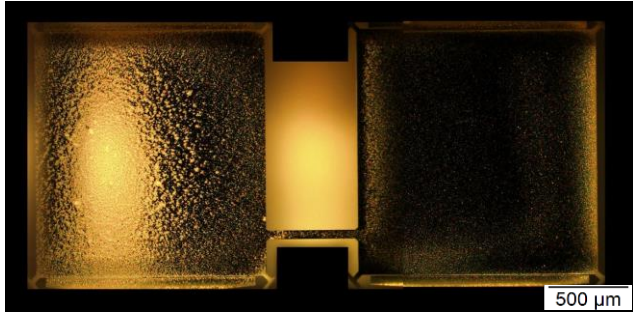


Fig. 7. Dark-field microscopic image of weakly coupled piezoelectric bulk acoustic MEMS resonators deposited with PSL particles on one of the resonators

The MEMS Impactor Stage has a nozzle arrangement which can be used for aligning the particle deposition on specific location in the resonator. The ultra-fine particles were deposited on resonator 1 by aligning the nozzle at the anti-nodal position of the Lamé mode to maximize the frequency-shift response. The frequency response of the coupled resonators was then measured individually for about 20 minutes at one-minute time intervals of deposition on resonator 1 in the open-loop.

## V. RESULTS AND DISCUSSION

With induced mass perturbation by depositing ultra-fine PSL particles (diameter of  $\sim 300$ nm) on resonator 1, the frequency response of the individual resonators (1&2) were plotted as shown in Fig. 8. and Fig. 9., respectively.

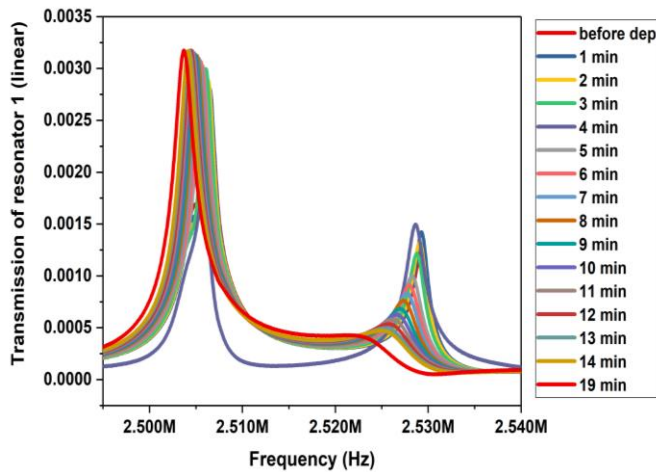


Fig. 8. Frequency response of resonator 1 over PSL deposition for 20 minutes on resonator 1 at one-minute time intervals

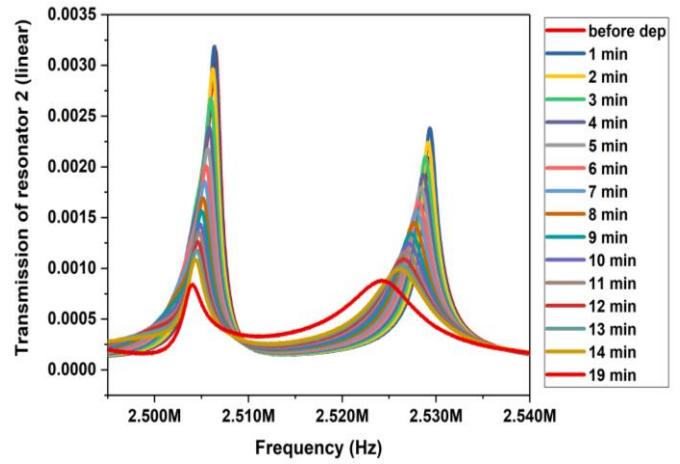


Fig. 9. Frequency response of resonator 2 over PSL deposition for 20 minutes on resonator 1 at one-minute time intervals

Fig. 8. and Fig. 9. showed that the frequency response of the resonators (1&2) shifted towards the negative direction for each one-minute time interval of mass deposition on resonator 1 throughout the 20 minutes deposition. The shift in resonant frequency for resonator 1 and 2 was observed considering the mode 1 at  $\sim 2.5$ MHz, before and after deposition. It should be noted that the shift in resonant frequency for both the resonators after 20 minutes deposition is only around 0.001% at mode 1.

Then the frequency response of the individual resonators was plotted after 20 minutes of deposition to compare the amplitude ratio relative to the frequency as shown in Fig 10.

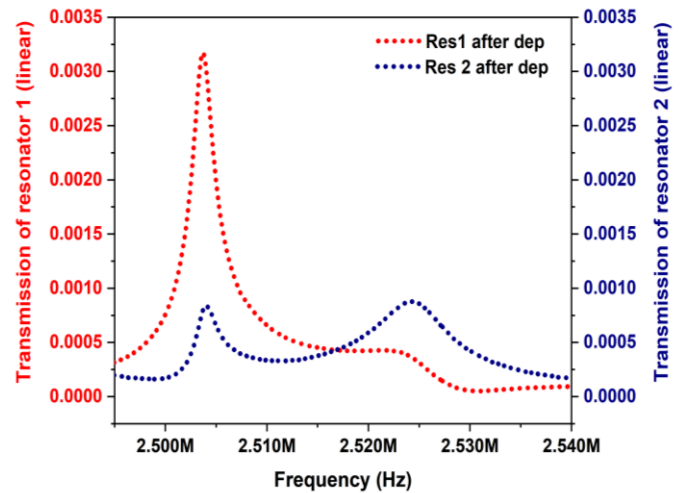


Fig. 10. Frequency response of resonator 1 and resonator 2 after 20 minutes deposition on resonator 1

It is evident from Fig. 10. that the amplitude of resonator 1 at mode 1 has significantly increased whereas the amplitude of resonator 2 at mode 1 has significantly decreased. This indicates that the vibration energy is confined to resonator 1 at mode 1 ( $\sim 2.5$ MHz) and corroborates the theory of mode localization as explained in section II. In order to obtain the sensitivity of this weakly coupled piezoelectric bulk acoustic

MEMS resonators to the ultra-fine particulates, the frequency shift response from one of the resonators and the amplitude ratio shift between the resonators was plotted as shown in Fig. 11. As expected, the measured amplitude ratio shift of the coupled resonators increases and demonstrated nearly three orders of magnitude improvement in parametric sensitivity for the PSL particles observed as shown in Fig. 11.

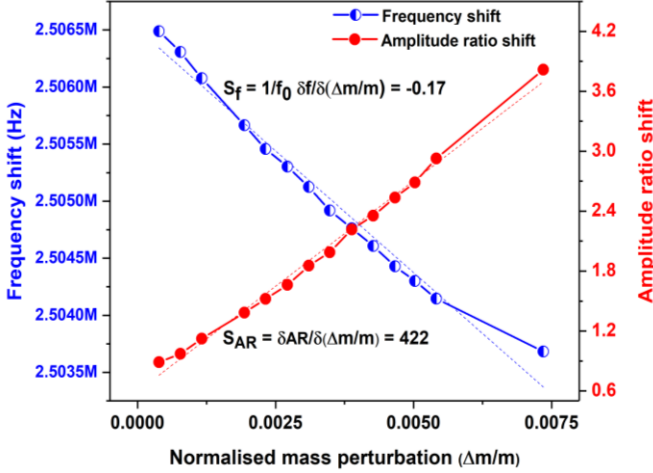


Fig. 11. Sensitivity of the weakly coupled resonators in terms of frequency shift and amplitude ratio shift

The frequency shift sensitivity and amplitude ratio shift sensitivity are given by the equations,

$$s_f = \frac{1}{f_0} \frac{\partial f}{\partial (\Delta m/m)} \quad (18)$$

$$s_{AR} = \frac{\partial (AR)}{\partial (\Delta m/m)} \quad (19)$$

The amplitude ratio shift data in Fig. 11. corresponds to the amplitude ratio between the resonators at mode 1 (~2.5 MHz). This in turn is comparable to that of the theoretical simulation obtained in Fig. 2. for a positive mass perturbation in one of the resonators and confirms vibration mode localization.

## VI. CONCLUSIONS

Weakly coupled MEMS resonators, exhibiting mode localization phenomena are shown to respond as highly sensitive mass sensors for ultra-fine PM measurement. A significant improvement in parametric sensitivity is seen when comparing the amplitude ratio readout metric to the resonant frequency shift. This feature in conjunction with the intrinsic common mode rejection properties offered by this transduction approach offers a promising route towards a portable platform for ultra-fine PM measurements.

## ACKNOWLEDGMENTS

The authors would like to acknowledge Arthur T. Zeilinski for the discussions on the MEMS Impactor Stage and particle deposition experiments.

## REFERENCES

- [1] A. T. Zeilinski, M. Kalberer, R. L. Jones, A. Prasad and A. A. Seshia, "Particulate mass sensing with piezoelectric bulk acoustic mode resonators," IEEE International Frequency Control Symposium, pp. 1-6, Sep. 2016.
- [2] J. P. Black, et al., "MEMS-Enabled Minutized Particulate Matter Monitor Employing 1.6 GHz Aluminum Nitride Thin-Film Bulk Acoustic Wave Resonator (FBAR) and Thermophoretic Precipitator," IEEE Ultrasonics Symposium Proceedings, pp. 476-479, December 2007.
- [3] E. Mehdizadeh, et al., "Aerosol impactor with embedded MEMS resonant mass balance for real-time particulate mass concentration monitoring," Int. Conf. Solid State Sensors, Actuators, and Microsystems, Barcelona, 2013.
- [4] H. S. Wasisto et al., "Partially integrated cantilever-based airborne nanoparticle detector for continuous carbon aerosol mass concentration monitoring," J. Sens. Sens. Syst., vol.4, pp. 111-123, 2015.
- [5] H. S. Wasisto, et al., "Airborne engineered nanoparticle mass sensor based on a silicon resonant cantilever," Sens. Actuators Chem., vol. 180, pp. 77-89, April 2012.
- [6] P. Thiruvankatanathan, J. Yan, and A. A. Seshia "Differential amplification of structural perturbations in weakly coupled MEMS resonators," IEEE Transactions on Ultrasonics, Ferroelectrics and Frequency Control, vol. 57, pp. 690-697, March 2010.
- [7] P. Thiruvankatanathan, J. Yan, J. Woodhouse, A. Aziz and A. A. Seshia "Ultrasensitive mode-localized mass sensor with electrically tunable parametric sensitivity," Applied Physics Letters, vol. 96, pp. 1-3, Feb 2010.
- [8] M. Spletzer, A. Raman, H. Sumali and J. P. Sullivan, "Highly sensitive mass detection and identification using vibration localization in coupled microcantilever arrays," Appl. Phys. Lett., vol. 92, March 2008.
- [9] Y. Wang et al., "A mass sensor based on 3-DOF mode localized coupled resonator under atmospheric pressure," Sens. Actuators Phys., vol. 279, pp. 254-262, Aug 2018.
- [10] A. Prasad, J. Charmet and A. A. Seshia, "Simultaneous interrogation of high-Q modes in a piezoelectric-on-silicon micromechanical resonator," Sens. Actuators Phys., vol. 238, pp. 207-214, Feb 2016.
- [11] M. Pandit et al., "Closed-Loop Characterization of Noise and Stability in a Mode-Localized Resonant MEMS Sensor," IEEE Transactions on Ultrasonics, Ferroelectrics and Frequency Control, vol. 66, pp. 170-180, October 2018.
- [12] A. Cowen, et al., "PiezoMUMPs TM Design Handbook," 2014.